Journal of the European Ceramic Society **13** (1994) 299–312

Microstructure and Mechanical Behaviour of Self-Reinforced Si_3N_4 and Si_3N_4–SiC Whisker Composites

F. Rossignol, P. Goursat, J. L. Besson

LMCTS, URA CNRS 320, 123 Av. A. Thomas 87060 Limoges, France

& P. Lespade

Aerospatiale, 33165 Saint-Medard-en Jalles, France

(Received 5 July 1993; accepted 20 September 1993)

Abstract

Monolithic Si_3N_4 and Si_3N_4–SiC whisker composites were fabricated by hot pressing or hot isostatic pressing. They were sintered in the 1600–1800°C temperature range with 6 wt% Y_2O_3 and 3 wt% Al_2O_3 as additives. Morphological aspects of whiskers were statistically determined by image analysis and different matrix microstructures were observed after chemical etching. Then, a correlation was established with mechanical properties.

When the same sintering conditions are used, the composite rupture stress increases or decreases with respect to that of the corresponding monolithic Si_3N_4 matrices. The increase is attributed to an effective load transfer mechanism which involves stress concentration at fibre–matrix interfaces. These interfaces can become the new critical defects in the microstructure when the whiskers are too large.

The resistance to short cracks was determined by indentation. The single edge precracked beam (SEPB) method allowed characterization of the resistance to long crack propagation. The toughness increases both with the aspect ratio of whiskers and/or elongated β-Si_3N_4 grains and with the precrack length (R-curve effect). The improvement is mainly due to the bridging of crack borders by acicular shapes or ligaments of unbroken matter. The R-curve corresponds to the enlargement of the active clamping zone as the crack extends. At a given precrack length the fracture toughness is strongly dependent upon the potential diameter of bridges, whereas the R-curve steepness rises with the density of clamping sites.

Monolithische Si_3N_4- und Si_3N_4/SiC-Whisker-komposite wurden durch heiß- oder heißisostatisches Pressen hergestellt. Die Komposite wurden bei Temperaturen zwischen 1600°C und 1800°C mit 6 Gew.% Y_2O_3 und 3 Gew.% Al_2O_3 gesintert. Morphologische Aspekte der Whisker wurden statistisch mit Hilfe der Bildanalyse bestimmt; nach dem chemischen Ätzen zeigten sich verschiedene Gefüge. Anschließend wurden die mechanischen Eigenschaften mit den Gefügen korreliert.

Bei Beibehaltung der Sinterbedingungen nimmt die Bruchbelastung bezüglich der jeweilgen Bruchbelastung der monolithischen Si_3N_4-Matrizen zu oder ab. Die Zunahme ist in einem effektiven Lasttransfer begründet, der Spannungskonzentrationen an der Faser–Matrix-Grenzfläche einschließt. Diese Grenzflächen können sich zu neuen, kritischen Defekten im Gefüge entwickeln, wenn die Whisker zu groß werden.

Die Bestimmung des Widerstands gegenüber kurzen Rissen erfolgte mit Hilfe von Härteeindrücken. Die SEPB-Methode erlaubt die Bestimmung des Widerstandes gegenüber der Ausbreitung langer Risse. Die Festigkeit nimmt sowohl mit dem Aspektverhältnis der Whisker und/oder der ellipsenförmigen β-Si_3N_4-Körner sowie mit der Länge des Startrisses zu (R-Kurven-Effekt). Diese Verbesserung ist hauptsächlich auf die Überbrückung der Rißflanken durch nadelförmige Verbindungen oder Reste ungebrochenen Materials zurückzuführen. Die R-Kurve entspricht einer Vergrößerung der aktiven Haftungszone während des Fortschreitens des Risses. Bei vorgegebener Länge des Startrisses hängt die Bruchfestigkeit hauptsächlich vom möglichen Durchmesser der Brücken ab, wohingegen die Steilheit der R-Kurve mit der Dichte der Haftbereiche steigt.

Journal of the European Ceramic Society 0955-2219/94/$7.00

Des monolithes Si_3N_4 et des composites à matrice Si_3N_4 reinforcée par des whiskers SiC sont fabriqués par frittage sous charge et compaction isostatique à chaud. Ces deux types de matériaux sont densifiés dans le domaine de température 1600–1800°C avec comme ajouts 6% en poids d'Y_2O_3 et 3% en poids d'Al_2O_3. Les paramètres morphologiques relatifs aux whiskers sont déterminés, de manière statistique, par analyse d'images. La révélation des microstructures matricielles est conduite par attaque chimique. Une corrélation vis-à-vis des propriétés mécaniques est alors établie.

Lorsque les conditions de frittage sont identiques, en fonction de la taille des whiskers, la contrainte à rupture des composites est soit supérieure soit inférieure à celle des monolithes. L'augmentation est attribuée à un mécanisme efficace de transfert de la charge appliquée sur les fibres. Néanmoins, ce mécanisme induit une concentration des contraintes aux interfaces fibres–matrices. Ces interfaces deviennent les nouveaux défauts critiques lorsque la taille des whiskers est trop importante et conduisent alors à une baisse de la contrainte à rupture.

La méthode d'indentation permet de calculer la ténacité relative à des fissures courtes. La méthode SEPB autorise l'évaluation de la ténacité sur des fissures de plus grande longueur. Les résultats montrent que cette ténacité s'accroît à la fois avec le facteur de forme des whiskers et/ou des grains β-Si_3N_4 aciculaires et avec la longueur de la préfissure (effet courbe-R). Ce phénomène est essentiellement dû au pontage des lèvres de la fissure par les formes aciculaires ou par des ligaments de matière non rompue. La courbe-R résulte de l'agrandissement de la zone active de pontage durant l'avancée de la fissure. Pour une longueur de préfissure donnée la ténacité dépend fortement du diamètre potentiel des ponts, tandis que l'acuité de la courbe-R dépend de leur nombre.

1 Introduction

Silicon nitride based ceramics are promising candidates for high temperature structural applications. The highly covalent Si–N bonds provide a favourable combination of chemical, mechanical and thermomechanical properties: hardness, high strength at high temperature (1400°C), low density (3·2 g/cm^2), low thermal expansion and good oxidation resistance. Many years of research have been concerned with providing reliable components comparable in quality to their metallic counterparts.[1] Dense products of Si_3N_4 are beginning to find commercial uses[2] such as roller followers, valves or turbocharger rotors in piston engines, but metal-cutting inserts continue to be the major commercial product. However, the fracture toughness of Si_3N_4 in the current state-of-the-art technology remains too low compared with those of metals to extend its development to spatial and aeronautic high-tech industries.

The first opportunity to enhance the resistance to crack propagation is the composite approach,[3,4] The incorporation of SiC whiskers to a Si_3N_4-based matrix allows dissipative mechanisms, such as crack bridging and crack deflexion, to operate and increase the work of fracture. The efficiency of these mechanisms is strongly dependent upon the size and the aspect ratio of the reinforcing whiskers and upon the strength of the fibre–matrix interface. Champion *et al.*[5] have reported strong *R*-curve effects in these composites. The understanding of the origin of the *R*-curve is crucial for the material in service. It controls both the flaw tolerance and the slow crack growth kinetics.

The second opportunity, mentioned by different authors, exploits the ability to obtain self-reinforced monoliths[6–9] (super-tough Si_3N_4). It is well known that due to the low self-diffusion coefficients in silicon nitride, densification necessitates sintering aids (MgO, Y_2O_3, Al_2O_3, Sc_2O_3, Li_2O, etc.) which react with silica always present on Si_3N_4 grains to form a eutectic.[10,11] So densification is based on liquid-phase sintering with dissolution of equiaxed α-Si_3N_4 initial grains and reprecipitation of β-Si_3N_4 acicular grains. As a consequence of their needle-like morphology, the β-phase grains can play a role similar to that of the SiC whiskers in composites. This opportunity, which does not occur in alumina,[12] has led some researchers to cast some doubt upon the interest of whisker addition to reinforce silicon nitride ceramics.[13,14]

The objective of the present study was to clarify the respective influences of nitride grain and SiC whisker morphologies on the mechanical properties. To this end, monoliths and composites have been fabricated by hot pressing or hot isostatic pressing. Different microstructures were achieved by changing the sintering temperature and were correlated to fracture strength and toughness. The results are discussed in the frame of current literature dealing with toughening in non-transforming ceramics.

2 Materials and Testing

2.1 Materials

Monoliths and composite matrices had the same nominal weight compositions to allow comparison tests. α-Si_3N_4 powder (UBE SNE-10) was mixed[15] with 6% Y_2O_3 (Lonza) and 3% Al_2O_3 (Rhône-Poulenc) as sintering aids. For the composites,

different types of silicon carbide whiskers (American Matrix (AM) and Atochem (ATO)) and two volume fractions (10% and 30%) were used. Thereafter the final material was shaped and densified by two methods.

- A reference route that included hot pressing (HP) in the temperature range from 1600°C to 1800°C, under a constant applied stress of 35 MPa and a duration of 2 h in N_2 atmosphere.
- The second process consisted in forming granulated premixed powders by cold isostatic pressing (CIP). Then, the glass encapsulated sample were outgassed and hot isostatically pressed (HIPped) for 3 h at 1700°C under 60 MPa.

To avoid complicated and long descriptions, the compositions of the samples will be labelled by the authors' own nomenclature. As an example, the specification of a material containing 30 vol.% of Atochem SiC whiskers, in a silicon nitride-based matrix sintered with 6 wt% Y_2O_3 and 3 wt% Al_2O_3, will be $30SiC_{ATO}$/S6Y3A. When it is necessary, the sintering method is also designated HP or HIP.

2.2 Microstructure of the matrix

The surfaces were ground and polished to a final 3 μm diamond paste. Chemical etching in molten soda was chosen among the various methods quoted in the literature[16,17] to reveal the microstructure of the matrix. Etching was conducted to lead to a removal of the intergranular phase sufficiently deep to reveal the morphology of the grains. This was slightly at the expense of the grain sizes themselves. Moreover, it is possible that soda preferentially attacks the α-phase and eliminates the smallest grains, increasing the apparent mean diameter. The surfaces were coated with carbon then gold to avoid charge effects during observations by SEM (JEOL JSM 35). Hot pressed materials were examined in a plane perpendicular to the hot pressing direction.

2.3 Morphological analysis of the whiskers

In contrast to the matrix, no etching was necessary to determine morphological aspects of SiC whiskers. Both the contrast between the whiskers and the matrix and the size of the whiskers were sufficient to obtain good optical micrographs from polished surfaces. These pictures were scanned, numerized and quantitatively analysed with a Macintosh software Optilab 2.0 from Graftek.

The objects on the observed surfaces were shape modelled as ellipses (see Fig. 1). An ellipse having the same long axis and the same surface as an object allows estimation of four parameters. The

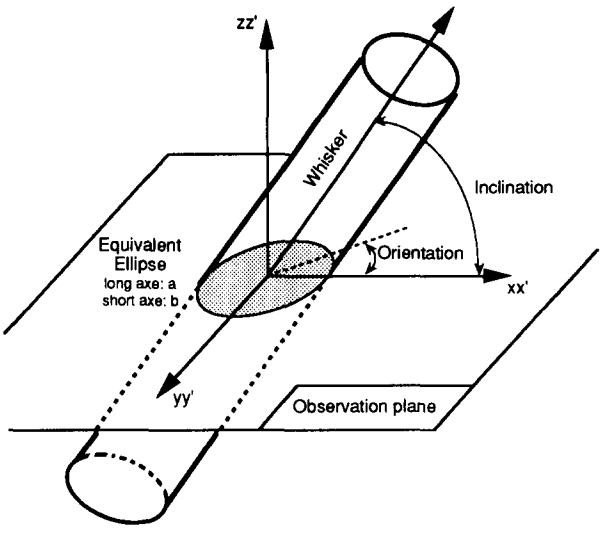

Fig. 1. Shape modelling for image analysis.

diameter of the whisker is equal to the short axis. The elongation factor in the considered plane corresponds to the ratio of the two axes. The in-plane orientation fits with that of the long axis. The fibre spatial inclination with respect to the observed plane is given by Arcsin(b/a) (see Fig. 1).[18] Four micrographs (600 to 1800 particles) were requested to build a statistically representative cumulated histogram for each parameter. Moreover, assuming that the coarsest whiskers play a greater role than the finest, the weight of a particle in the statistics has been pondered with a factor given by the surface of the particle over the total particle surface. It was possible to compare the resulting pondered histogram, which was supposed to be close to the reality, to the basic one.

In order to take into account the effect of the densification method, hot pressed samples were analysed on two different views: one perpendicular and the other parallel to the applied sintering stress. Hipped materials were not submitted to image analysis but simply qualitatively examined. It must be noticed that the parameters were measured in two dimensions, not in three. However, the difference between what could be called an apparent measure and the 3D reality was only significant for the elongation factor. Eventually this apparent elongation factor represented the more efficiency one for a crack advancing perpendicular to the observed plane, according to the different models of reinforcement by bridging.[19,20]

2.4 Phase analysis

The diffraction patterns were obtained with a Philips PW 1729 apparatus equipped with a copper anticathode. Samples were analysed in a massive form.

Since, for the hot pressed samples, the irradiated plane was always taken perpendicular to the sintering direction, it was considered that the probable

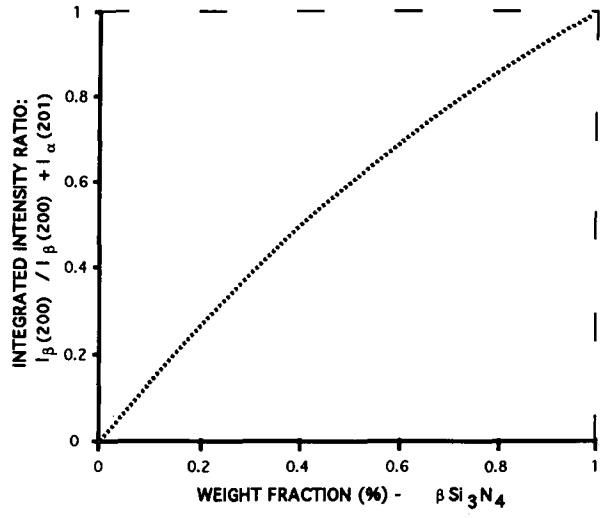

Fig. 2. Calculated calibration curve for quantitative XRD analysis.

microstructure orientation effects[17] on the X-ray diffraction output were constant. That is why semi-quantitative and comparative determinations of the β-Si_3N_4/α-Si_3N_4 ratio have been made first on monolithic hot pressed materials using the integrated intensity of the pick [200] for β-Si_3N_4 and [201] for α-Si_3N_4. The ratio has been corrected according to the calculated calibration curve, shown in Fig. 2, which was derived from the procedure developed by Gazzara & Messier.[21] No internal standard was used. The main goal was to estimate the effect of sintering temperature on the $\alpha \rightarrow \beta$ transformation rather than to measure very precisely the β/α value.

This determination has also been used for the composites assuming that the presence of a silicon carbide phase does not basically modify the ratio between β- and α-silicon nitride peaks. In other words, the crystallographic structure of SiC, similar to that of silicon nitride, does not give rise to fluorescence phenomena, as silicon does, for instance.[22]

2.5 Mechanical testing

The fracture strengths were determined at room temperature on a three-point bend fixture with a span of 19 mm and at a crosshead speed of 0·2 mm/min. The tested bars had a cross-section of 3 mm high by 4 mm wide. Their prospective tensile faces were polished up to 3 μm and edges bevelled to eliminate machining defects. The hot-pressed samples were tested in the hot pressing direction. Each mean value of rupture stress was calculated from eight experiments that ensure an accuracy better than 6%.[23]

On the one hand, the short crack resistance of each material was explored by the indentation fracture method. It was conducted on diamond polished surfaces with a Vickers microhardness indenter under an applied load of 295 N. The hot pressed monoliths and composites have been indented on a plane perpendicular to the hot pressing direction. From optical measurement of the generated crack size, the fracture toughness was calculated using the formula of Evans & Charles.[24] It must be kept in mind that a lot of formulae are proposed in the literature,[25] each leading to different toughness values. Consequently, indentation techniques provide only a basis for comparison.

On the other hand, the single edged precracked beam method[26] was used to characterize the resistance to long crack propagation. The test bars were 4 mm high (w) by 3 mm wide. The precrack length (a) was adjusted in a range from 1 mm to 3 mm ($0{\cdot}25 < w/a < 0{\cdot}75$). The precracked samples were submitted to flexure on a three-point bend fixture with a span of 16 mm and at a crosshead speed of 0·2 mm/min. Hot pressed specimens were fractured in the hot pressing direction. The fracture toughness was calculated using the formula of Srawley.[27] This method has already been successfully employed in the case of several monoliths and composites and gives reproducible values.[28]

3 Results and Discussion

3.1 Densification

Hot pressed monoliths reach their maximum density as early as 1600°C (see Fig. 3). This temperature goes up to 1650°C in the case of composites because the whiskers act as rigid inclusions, impeding the sintering mechanisms.[29,30] When the sintering temperature increases, a slight densification decrease appears, especially for monoliths. It can be attributed to both the decomposition onset of silicon nitride promoted by the great quantity of eutectic liquid phase and the growth of an acicular microstructure, as will be discussed

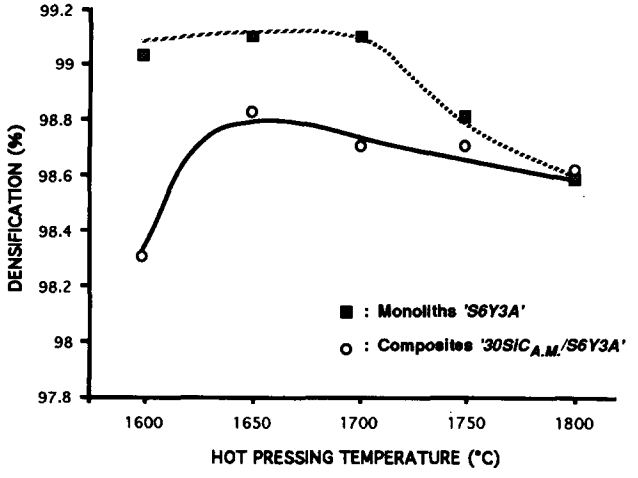

Fig. 3. Influence of the hot pressing temperature on the densification.

Table 1. Influence of the whisker morphology and volume fraction and the sintering method on the densification

Materials	Sintering	Densification (%)
$30SiC_{AM}$/S6Y3A	HIP at 1700°C	98·8
$10SiC_{AM}$/S6Y3A	HP at 1730°C	99
$30SiC_{AM}$/S6Y3A	HP at 1730°C	98·7
$30SiC_{ATO}$/S6Y3A	HP at 1730°C	99·7

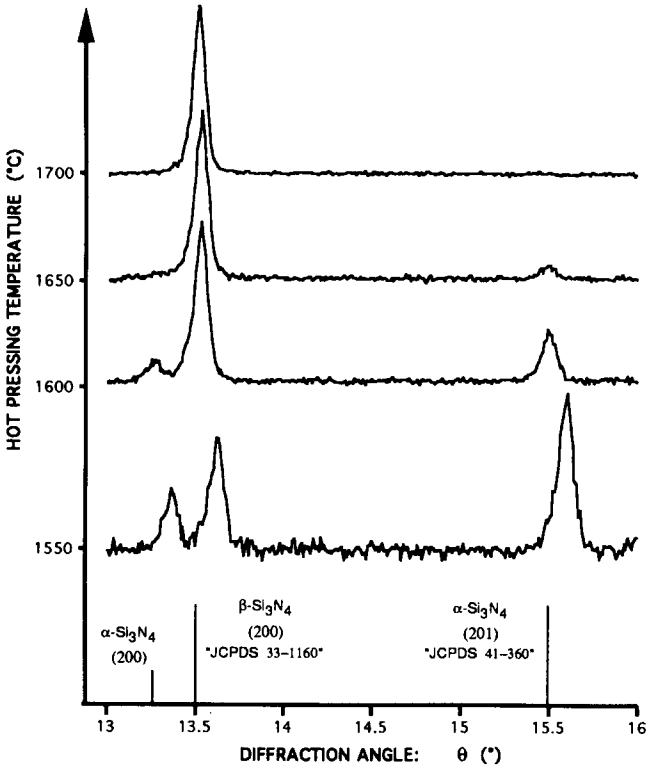

(a)

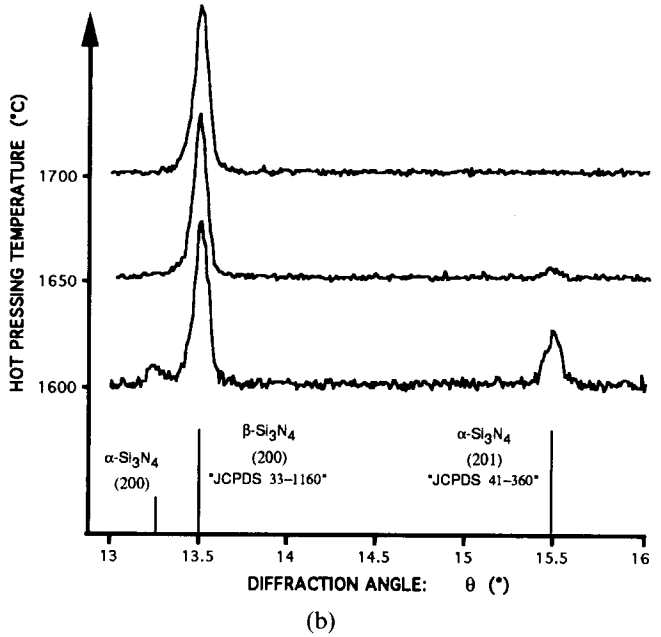

(b)

Fig. 4. XRD patterns of (a) S6Y3A monoliths and (b) $30SiC_{AM}$/S6Y3A composites hot pressed at different temperatures. λ_{Cu} = 0·15406 nm.

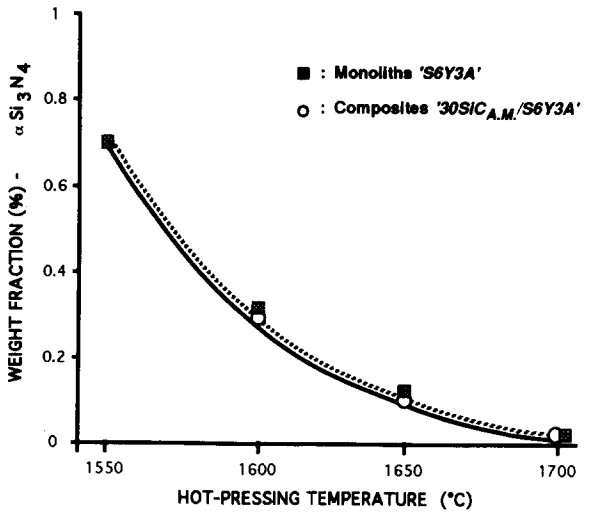

Fig. 5. Influence of the hot pressing temperature on the $\alpha \rightarrow \beta$ transformation.

later. The rigid skeleton of the fibres limits this effect in the composites. Actually the residual porosity always remains very low (see Table 1).

X-Ray analysis established that the α-Si_3N_4-β-Si_3N_4 transformation was complete as early as 1700°C whatever the samples (see Fig. 4(a) and 4(b)). The presence of the whiskers did not modify the kinetics of the transformation (see Fig. 5).

3.2 Microstructure

Figure 6(a) already shows a great proportion of β acicular grains in monoliths hot pressed at 1600°C, which is in total agreement with X-ray measurements. Their apparent mean diameter increases by a factor 4 from 1600°C to 1800°C (see Fig. 6(a) to (c)).

In composites, the presence of whiskers, whatever their sizes, does not significantly affect the

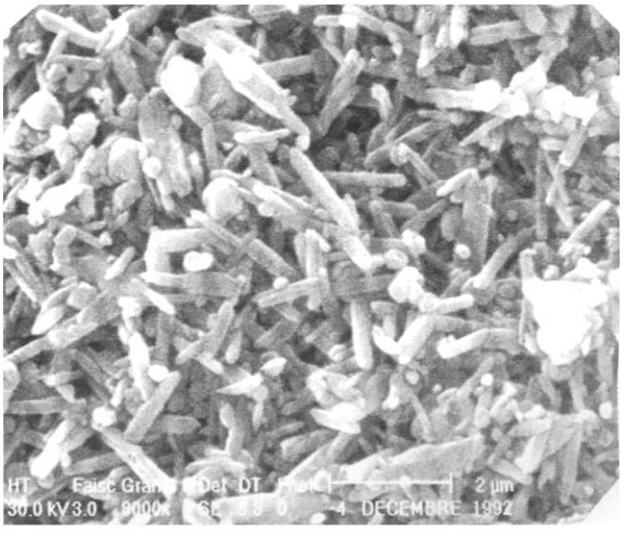

(a)

Fig. 6. Monoliths S6Y3A hot pressed at (a) 1600°C, (b) 1700°C, (c) and (d) 1800°C; (e) composites $30SiC_{AM}$/S6Y3A hot pressed at 1800°C; (f) composites $30SiC_{ATO}$/S6Y3A hot pressed at 1730°C; (g) composites $30SiC_{AM}$/S6Y3A hot isostatically pressed at 1700°C.

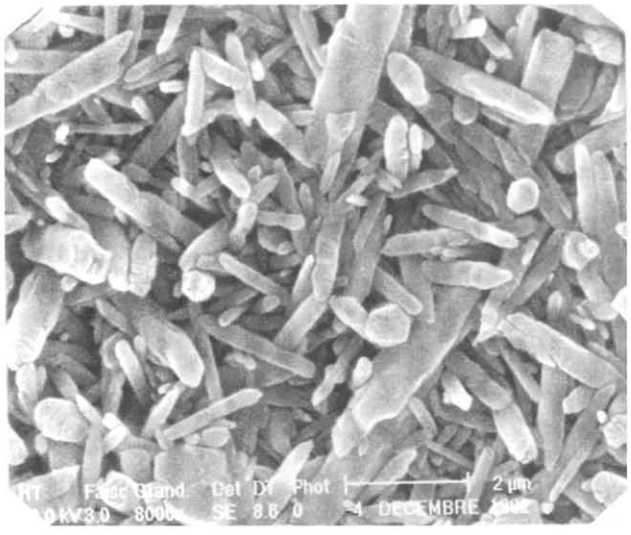

(b)

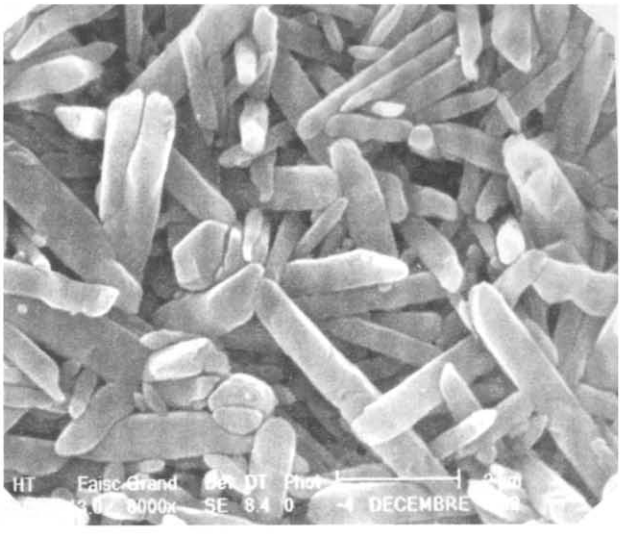

(c)

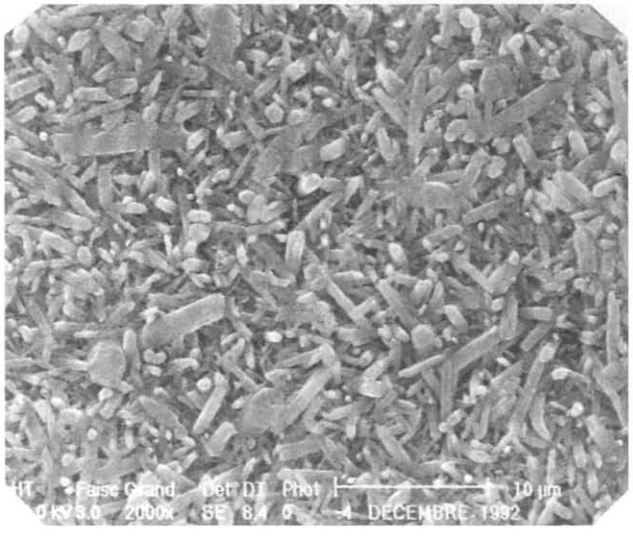

(d)

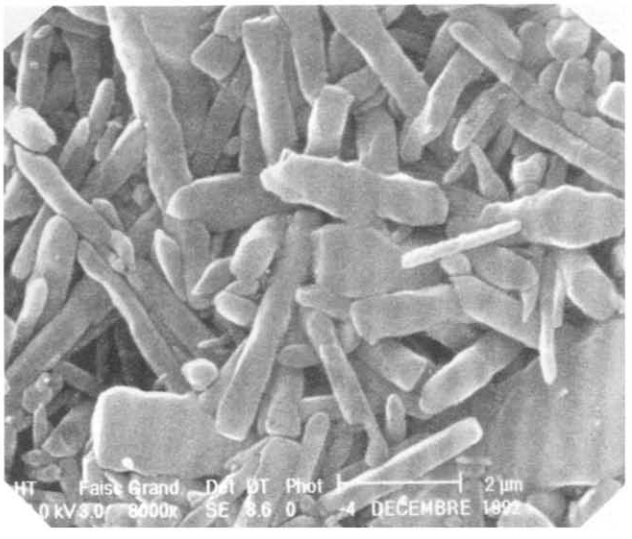

(e)

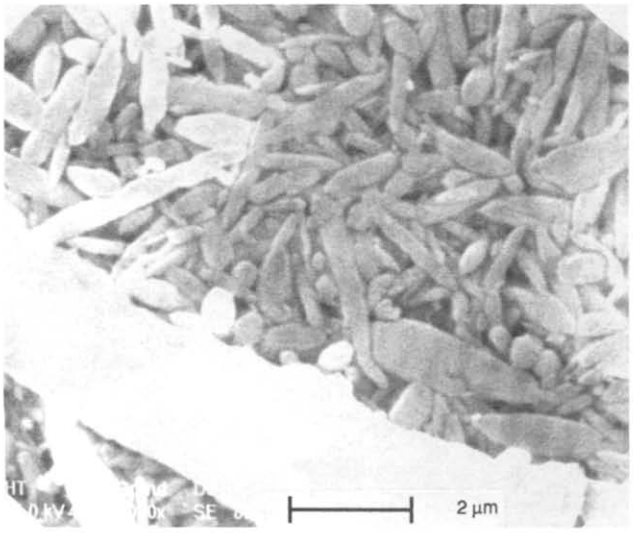

(f)

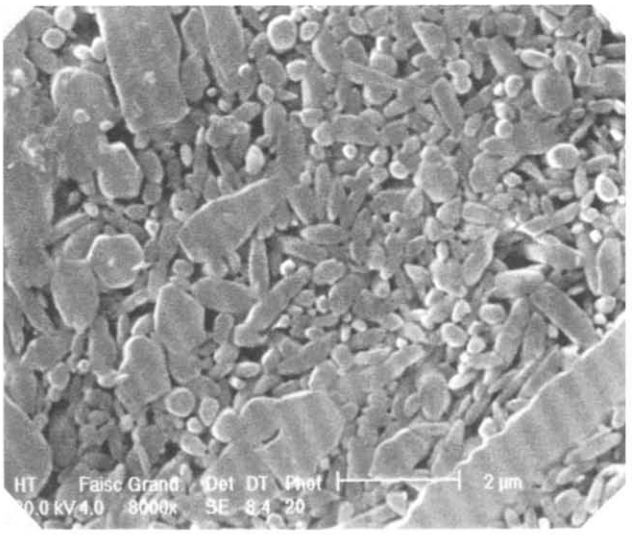

(g)

Fig. 6.—*contd.*

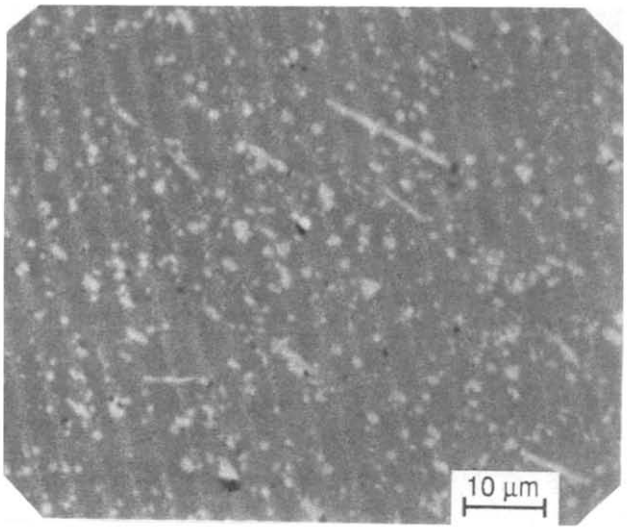

(a)

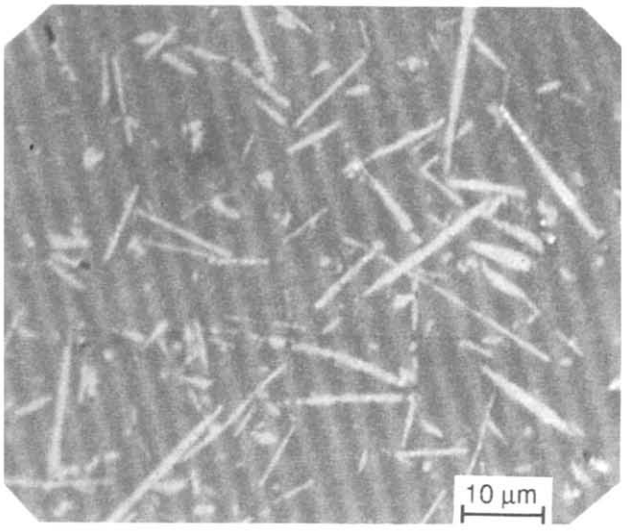

(b)

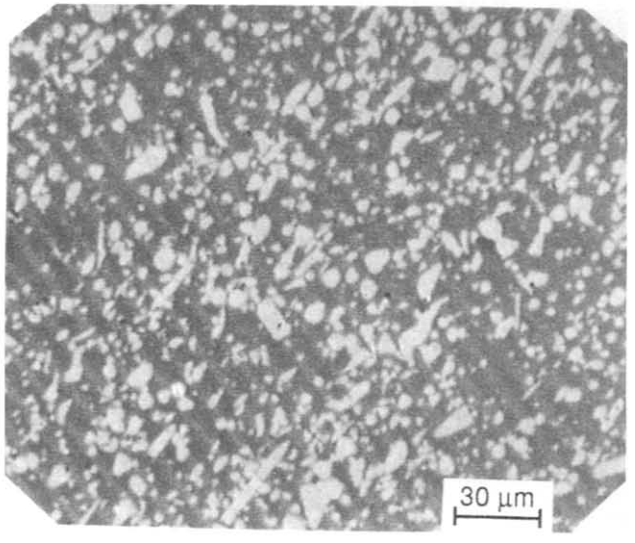

(c)

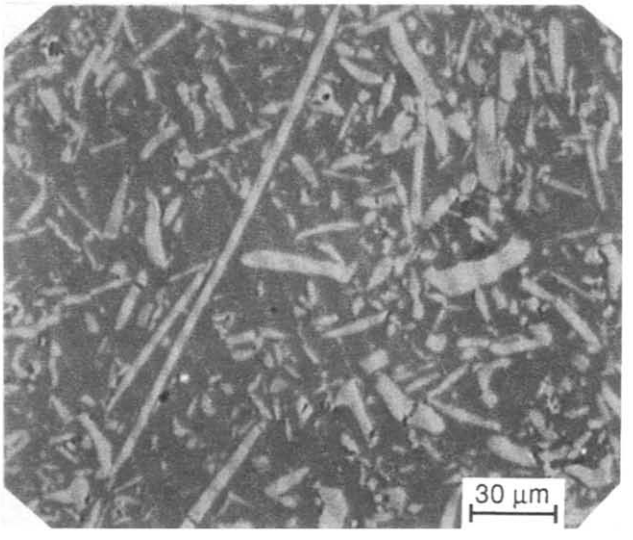

(d)

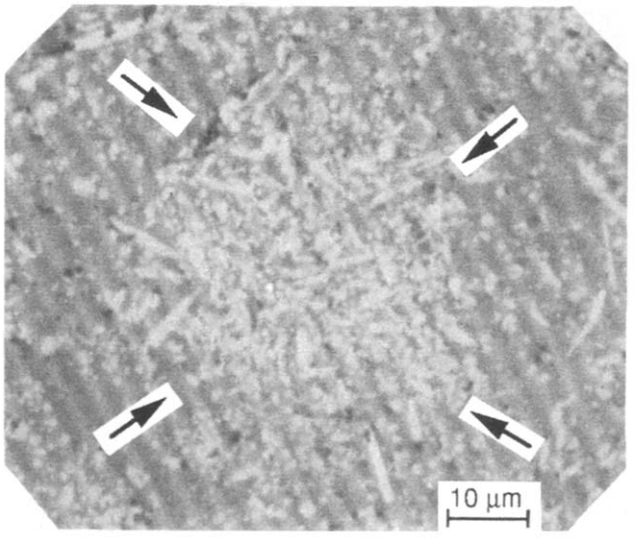

(e)

Fig. 7. Composites $10SiC_{AM}$/S6Y3A hot pressed at 1730°C. Details of a polished surface (a) parallel and (b) perpendicular to HP direction. Composites $30SiC_{ATO}$/S6Y3A hot pressed at 1730°C. Details of a polished surface (c) parallel and (d) perpendicular to HP direction. Composites $30SiC_{AM}$/S6Y3A hot isostatically pressed at 1700°C. Details of a polished surface (whisker nest).

Table 2. Image analysis results—mean values and standard deviations

		Observed plane/HP direction and composite type			
		Parallel $10SiC_{AM}/S6Y3A$	Parallel $30SiC_{ATO}/S6Y3A$	Perpendicular $10SiC_{AM}/S6Y3A$	Perpendicular $30SiC_{ATO}/S6Y3A$
Diameter	Real (μm)	0·8 (0·4)	2·2 (1·3)	0·9 (0·5)	2·2 (1·4)
	Pondered	1·3 (0·6)	3·7 (1·6)	1·6 (0·7)	4·2 (1·9)
Elongation factor	Real	1·9 (0·7)	2 (0·7)	3·2 (2·5)	3·1 (2·1)
	Pondered	2·2 (1·1)	2·2 (0·9)	6·8 (5·7)	5·8 (4·4)
Inclination	Real (°)	47 (28)	38 (22)	42 (31)	36 (27)
	Pondered	28 (18)	28 (11)	16 (22)	15 (12)
Orientation	Real (°)	97 (59)	93 (43)	89 (50)	95 (52)

microstructure of the matrix (compare Fig. 6(c)/(e)) and (b)/(f)).

It must be noticed that in monoliths hot pressed at 1800°C, coarsening results in acicular grains which can be compared in size with the AM whiskers. Moreover, some of them have grown exaggeratedly, giving a bimodal microstructure (see Fig. 6(d)).

In return, for HIPped samples, lower grain sizes and aspect ratios are observed, grain growth being inhibited by the high pressure (60 MPa) (see Fig. 6(g)).

Figures 7(a) to (d) show the typical skeleton of AM and ATO whiskers in hot pressed materials. For image analysis, these optical micrographs were enlarged. Table 2 and Fig. 8(a) to (d) sum up the image analysis results and their exploitation. The AM and ATO whiskers have the same elongation factor when observed in corresponding sections with respect to the hot pressing direction (see Fig. 8(b)). In the two cases, fibres are mainly dispersed isotropically with the exception of the biggest ones (see Fig. 8(c) and (d)). These big whiskers, which are also the more efficient, are at a mean 15° angle to the pressing plane. This result is consistent with a previous work.[5]

In contrast, the two sources of whiskers differ in mean diameter and associated statistical distribution (mean diameter: 0·8 μm for AM whiskers with a narrow distribution; 2·2 μm for ATO whiskers with a large distribution) (see Fig. 8(a)).

In the particular case of HIPped samples, whisker nests are often observed and image analysis is difficult to perform (see Fig. 7(b)).

Table 3. Influence of the whisker morphology and volume fraction and the sintering method on the fracture strength—mean values and standard deviations

Materials	Sintering	Fracture strength (MPa)
$30SiC_{AM}/S6Y3A$	HIP at 1700°C	550 (30)
$10SiC_{AM}/S6Y3A$	HP at 1730°C	860 (80)
$30SiC_{AM}/S6Y3A$	HP at 1730°C	950 (70)
$30SiC_{ATO}/S6Y3A$	HP at 1730°C	680 (50)

In short, the silicon nitride grains of monoliths and composite matrices have practically the same size and morphology when they are fabricated in the same way, which means that the whiskers do not inhibit the grain growth. At a given volume fraction of whiskers in composites, there are less ATO whiskers than AM and the spacing between them is more important.

3.3 Inherent flaws—rupture strength

When the maximum density is reached, at 1600°C for hot pressed monoliths and at 1650°C for hot pressed composites, the rupture strength is not dependent upon the sintering temperature (see Fig. 9). It means that the defect populations are similar.

According to the whisker size and volume fraction, an increase or a decrease is observed with respect to the rupture strength of the corresponding silicon nitride matrices (see Table 3). The fibre–matrix bond is strong enough to provide an effective load transfer. The ultimate strength data show that the transfer is very efficient with AM whiskers but remains fairly good with ATO whiskers.

For a monolith hot pressed at 1730°C, having a toughness of 6 $MPa\sqrt{m}$ (as will be reported later) and a rupture strength of 800 MPa, the size of the critical defect, assuming a half-penny shape ($K_c = Y\sigma\sqrt{a_c}$ with $Y = 1{\cdot}3$), is about 30 μm. The addition of whiskers is beneficial in the way they limit the potential size of the matrix defects. The mean distance between the fibres has been evaluated at 20 μm for ATO composites and less for AM composites (Rossignol, F., *et al.*, unpublished). However, an effective load transfer involves stress concentrations at the fibre–matrix interfaces. These interfaces become the new potential defects in the microstructure and when the whiskers are too big, the transfer is over-compensated by the increase of the defect size.[31] In the case of HIPped materials (see Table 3), the lower mean fracture strength (550 MPa) is due to the presence of whisker nests (see Fig. 7(e)).

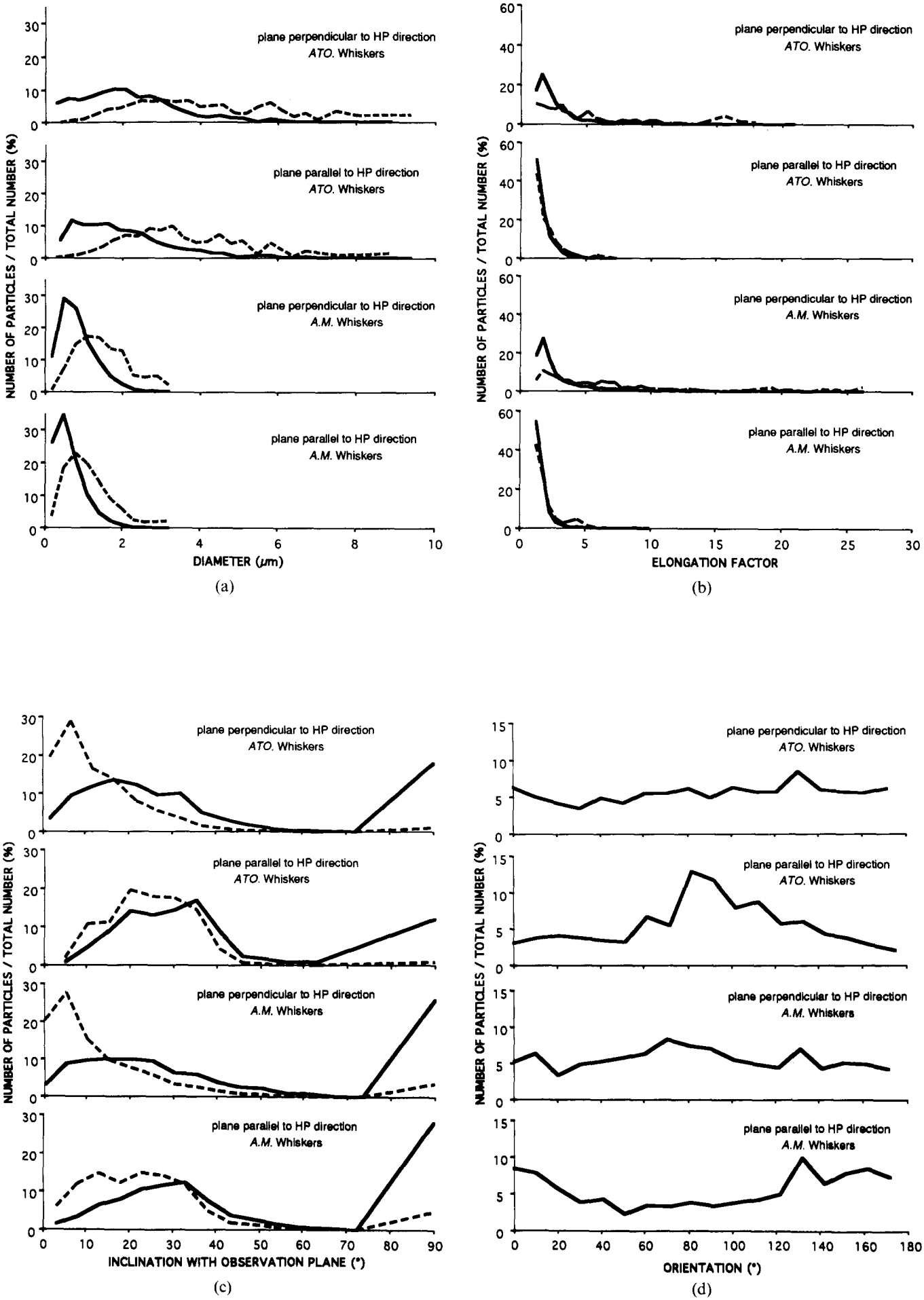

Fig. 8. Morphological analysis of the whiskers in $10SiC_{AM}$/S6Y3A and $30SiC_{ATO}$/S6Y3A composites hot pressed at 1730°C. (a) Diameter, (b) elongation factor, (c) inclination with observation plane; (d) orientation versus number of particles/total number; ——, real distribution; – – – –, pondered distribution.

Table 4. Influence of the whisker morphology and the sintering method on the indentation fracture toughness—mean values and standard deviations

Materials	Sintering	Indentation fracture toughness (MPa $\sqrt{m}$)
$30SiC_{AM}$/S6Y3A	HIP at 1700°C	6·4 (1·2)
$30SiC_{AM}$/S6Y3A	HP at 1730°C	6·8 (0·9)
$30SiC_{ATO}$/S6Y3A	HP at 1730°C	8·2 (0·6)

3.4 Resistance to short cracks introduced by indentation

The fracture toughness measurements are reported in Table 4 and Fig. 10(a) and 10(b). Each value has been calculated from 40 measurements. The high standard deviation, about 1 MPa$\sqrt{m}$, is due to several reasons: first the measure is local because the volume affected by the indentation remains small towards the heterogeneity scale of the materials (see Fig. 10 (c)); secondly the theoretical treatment by Evans & Charles does not take crack sinuosity into account; finally it is always very difficult to precisely localize the tip of the generated crack.

In hot pressed monoliths, a first increase in fracture toughness happens when the sintering temperature is increased from 1600°C to 1650°C, which corresponds to the temperature at which the $\alpha \rightarrow \beta$ transformation becomes complete. Sintering above 1700°C induces a further but limited increase in toughness.

In contrast, the fracture toughness of AM hot pressed composites is constant as soon as the maximum density is reached, at about 1650°C. The toughness of monoliths, sintered at 1800°C, reaches that of AM composites.

It is now well documented[32] that in non-transforming ceramics, fracture toughness can be improved by the incorporation of a second phase such as whiskers, grain size effects or the development of elongated matrix grains, which give rise to dissipative mechanisms in the crack wake. These dissipative mechanisms might be deflection of the crack tip and crack bridging by elongated phases that impose a closure stress between the crack borders, debonding and frictional sliding during crack opening.

The micrographs (see Fig. 10(d) and (e)) show, in the case of the composites, that crack deflections at the whisker–matrix interface and crack bridgings by whiskers and ligaments of matter are operating simultaneously. Toughness being independent from sintering temperature, it can be inferred that the whiskers play the major role in the improvement of toughness. For monoliths, the first increase in toughness is associated with the development of a fully β acicular structure. According to Matsuhiro & Takahashi[33] a minimal

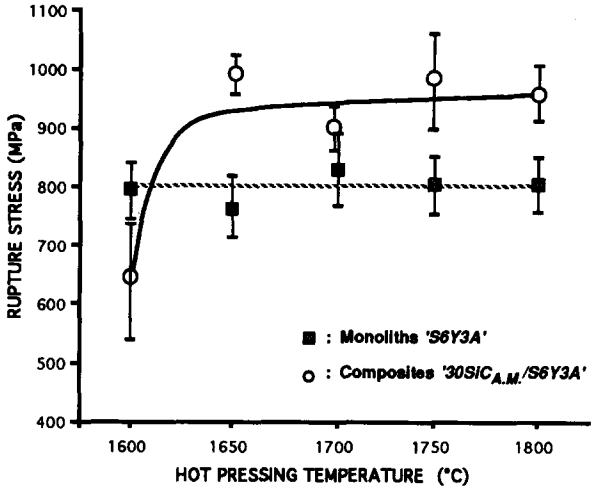

Fig. 9. Influence of the hot pressing temperature on the fracture strength.

diameter of about 1 μm is required for the elongated Si_3N_4 grains to contribute to the toughening. As the sintering temperature is raised the population of Si_3N_4 grains satisfying this condition increases, and after sintering at 1800°C the toughening is equal to that obtained with 30 vol.% of AM SiC whiskers. Due to their greater strength, the critical diameter for the SiC whiskers is smaller than that required for the β-Si_3N_4 grains of the matrix, as is demonstrated by their effective role in improving toughness.

In ATO composites whereas the whiskers are more spaced, so that the number of interactions between the crack and the fibres is smaller, the indentation toughness is higher. The toughness decrement due to a larger whisker spacing is compensated by the increase in the fracture energy of the whiskers. This emphasises the pre-eminent role of the whisker diameter.

For AM HIPped composites the toughness is only 5·5 MPa$\sqrt{m}$. Both the whisker agglomerates and the finer matrix texture diminish the bridging and deflection effects.

3.5 Resistance to long crack propagation—single edge precracked beam (SEPB) method

Whatever the materials under study, fracture toughness increases with precrack length (see Fig. 11(a) to (d)). According to Nose and Fujii,[34] the SEPB method yields K_{IC} values almost equal to those measured by the single-edge fatigue-cracked beam method prescribed in ASTM-E399-Annex 3 in the case of Al_2O_3 material. The authors have verified that the SEPB method, applied to a coarse grain alumina (A123 from Degussa) leads to results that are consistent with those reported by Wieninger *et al.*[35] for the same grade of alumina using the fatigue method. Such an increment in toughness is considered to be an *R*-curve behaviour. In the absence of phase transformation

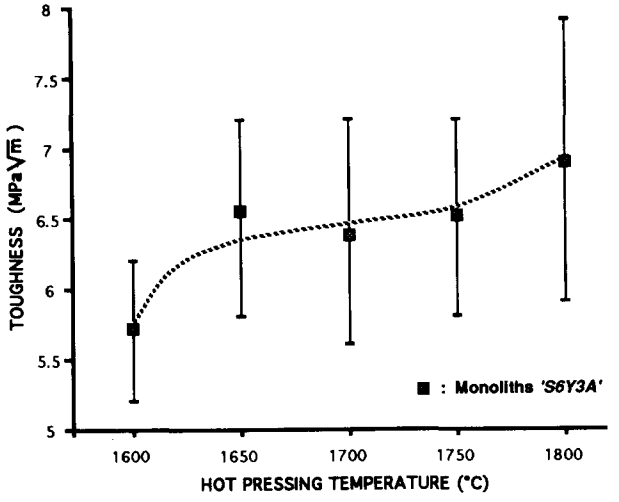

(a)

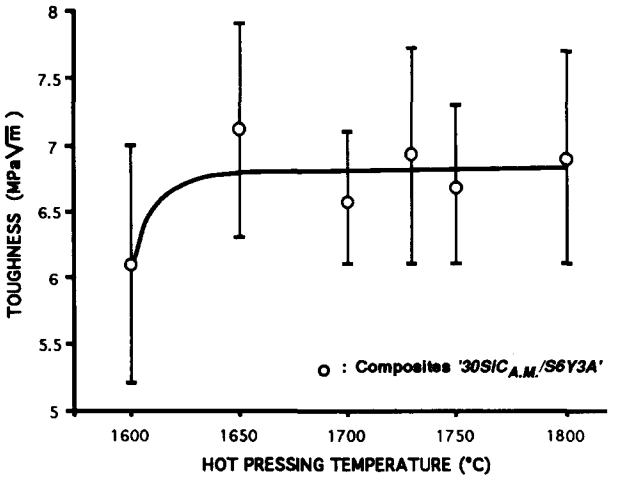

(b)

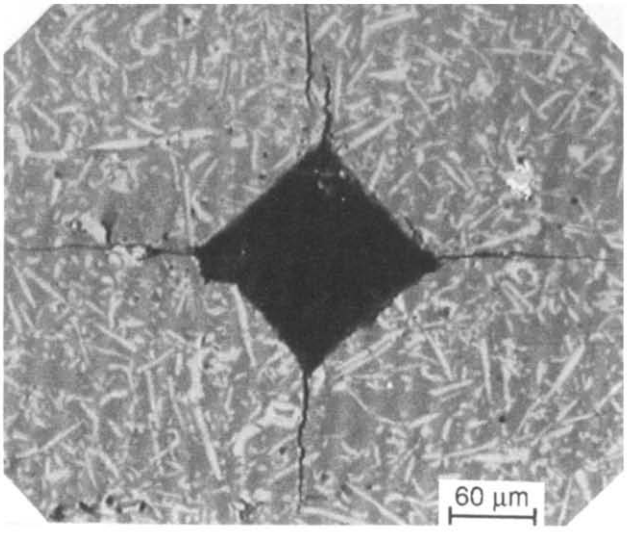

(c)

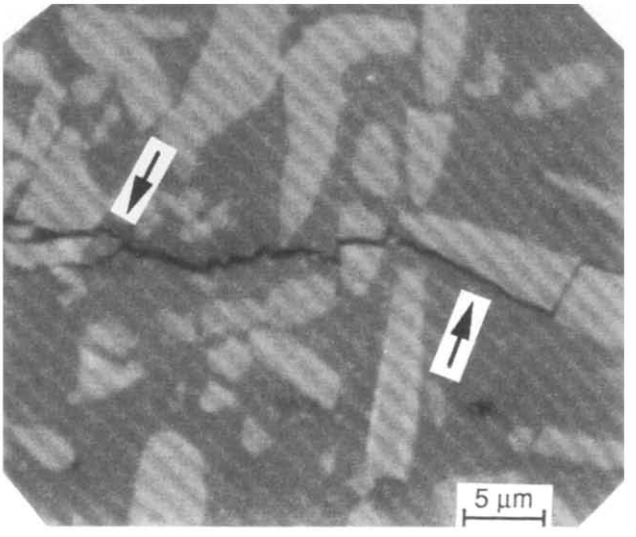

(d)

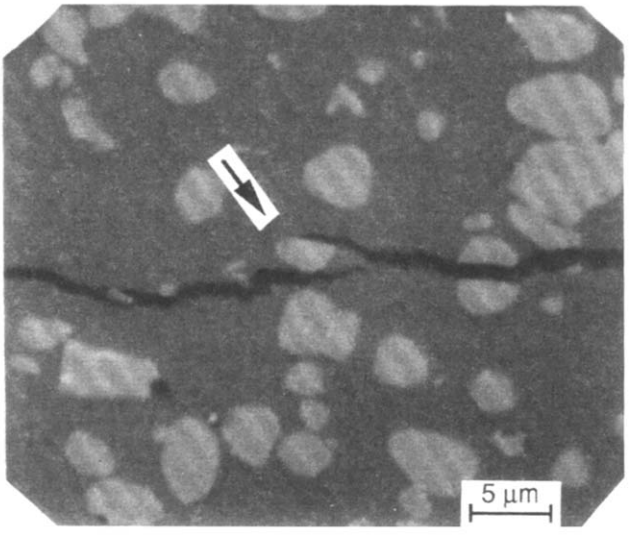

(e)

Fig. 10. Influence of the hot pressing temperature on the fracture toughness; (a) monoliths S6Y3A; (b) composites $30SiC_{AM}$/S6Y3A. (c) Composites $30SiC_{ATO}$/S6Y3A hot pressed at 1730°C. Indentation scale/microstructure. Indentation on composites $30SiC_{ATO}$/S6Y3A hot pressed at 1730°C. Details of the crack wake: (d) ligament and deflexion; (e) ligament.

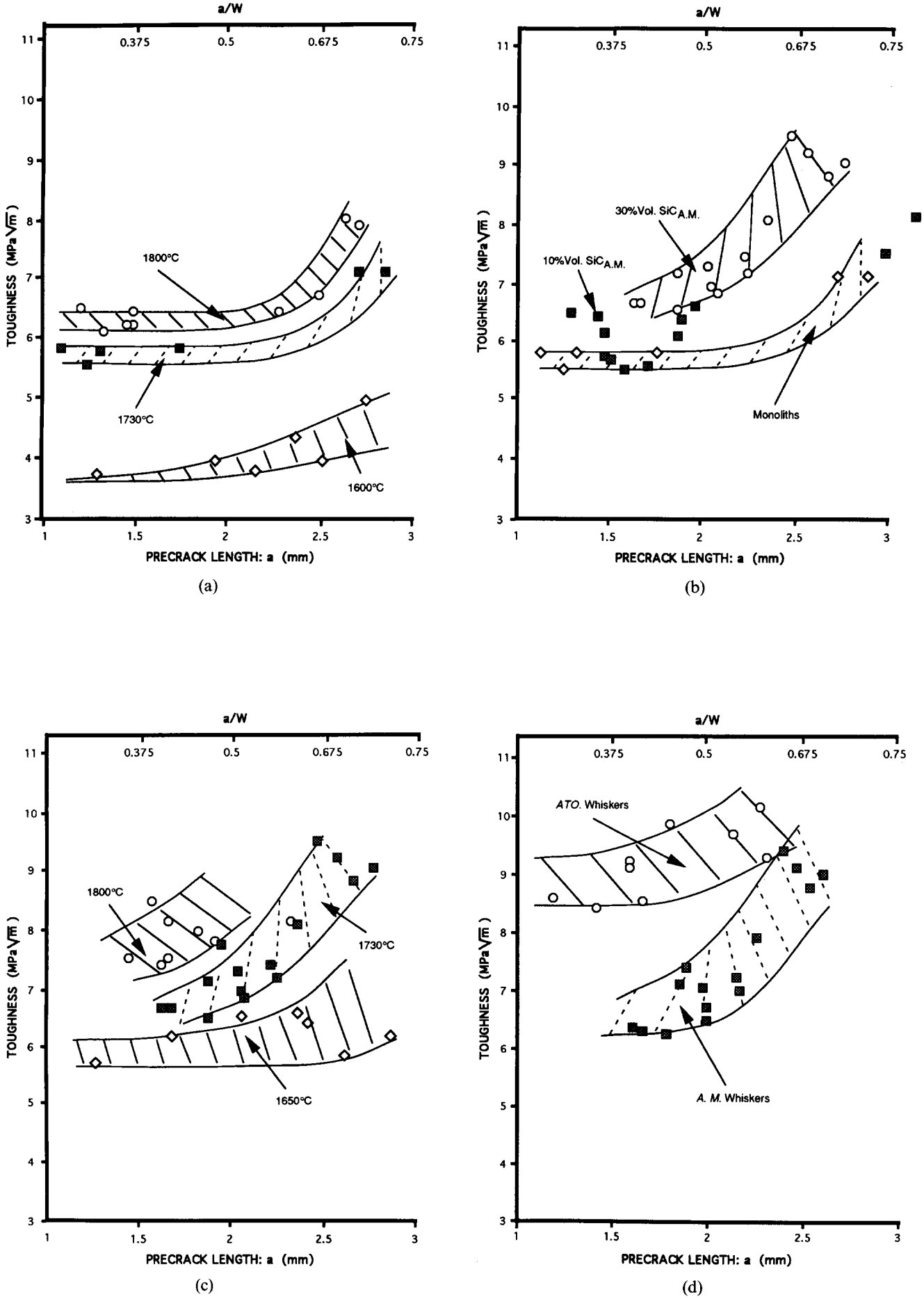

Fig. 11. (a) Influence of the hot pressing temperature on the SEPB fracture toughness of S6Y3A monoliths; (b) Influence of the whisker volume fraction on the SEPB fracture toughness of SiCAM/S6Y3A materials hot pressed at 1730°C; (c) Influence of the hot pressing temperature on the SEPB fracture toughness of 30SiCAM/S6Y3A composites; (d) Influence of the whisker morphology on the SEPB fracture toughness of 30SiC/S6Y3A composites hot pressed at 1730°C.

on the front of the advancing crack and of microcracking around the crack tip, the increase in crack resistance must be attributed to crack border interactions. The active mechanisms are the same as those identified and already discussed for short cracks from microstructural details of the crack wake profile (Fig. 10(d) and (e)). The *R*-curve effect is due to the enlargement of the zone of adhesion and friction in the wake of the actual crack tip as the crack extends. One must note the absence of any firm indication that the toughness has reached a plateau over the crack size range covered. A similar behaviour was observed by Braun *et al.*[36] in their study on alumina-based ceramics.

According to Choi & Salem,[14] silicon nitride with equiaxed grains does not exhibit any *R*-curve behaviour. In the present work, for monoliths hot pressed at 1600°C (see Fig. 11(a)), a slightly increased toughness is observed versus the precrack length. As the sintering temperature increases, so does toughness; there is a trend to a steeper *R*-curve. The low *R*-curve effect in the former case is due to the presence of 30 vol.% of equiaxed fine grains that do not participate to the toughening. When the $\alpha \rightarrow \beta$ transformation is complete, the entirely acicular structure is more efficient. The steeper curves observed with rising sintering temperature are related to the increase in diameter of the needle-like grains. A similar behaviour has been reported by Steinbrech[37] for long crack tests in alumina. Braun *et al.*[36] have observed and modelled a similar trend on alumina-based ceramics using indentation flaws.

The addition of SiC whiskers (see Fig. 11(b)) plays in a composite the same role as acicular grains. A composite with 10 wt% of AM whiskers and hot pressed at 1730°C leads to the same characteristics as those of the super-tough Si_3N_4 hot pressed at 1800°C. The improvement due to the whiskers increases with the whisker content.

Figure 11(c) demonstrates that the contribution of the whiskers may be enhanced by a contribution from the matrix, resulting in a synergistic effect.

As predicted by the model of Becher *et al.*,[19] the bigger size of ATO whiskers provides stronger clamping forces between the crack borders and are very efficient in obtaining materials with very high toughness. However, at a given volume fraction, the number of clamping sites is lower and the *R*-curve effect is less pronounced.

4 Conclusion

Monolithic Si_3N_4 and Si_3N_4–SiC whisker composites were fabricated by hot pressing or hot isostatic pressing in the temperature range 1600–1800°C with 6 wt% Y_2O_3 and 3 wt% Al_2O_3.

The $\alpha \rightarrow \beta$ transformation is not affected by the presence of SiC whiskers and is complete for a sintering temperature of 1700°C. The coarsening of the acicular β grains occurs mainly above 1700°C and a noticeable fraction of them becomes comparable in size with AM whiskers.

By image analysis, the in-plane aspect ratio of the reinforcement is found equal for the two fibre grades but the diameter of the ATO whiskers is three times that of the AM ones. Even after hot pressing, the whiskers are isotropically distributed, except for a fraction of them formed by the biggest ones which tend to lie in the pressing plane.

The ultimate strength of the composites is high. It is the result of a fairly good load transfer. Whereas the whiskers have a beneficial effect in limiting the size of the matrix defects, a new population of defects arises from the stress concentration at the fibre–matrix interface. So, either an increase or a decrease of the ultimate strength is observed with respect to monoliths.

The resistance to long crack propagation, determined by the SEPB method, shows that the toughness rises with the size of the whiskers and the aspect ratio of the elongated β-Si_3N_4 grains, and with the precrack length. The bridging of the crack borders by acicular shapes or ligaments of unbroken matter is one of the main reinforcement mechanisms. The *R*-curve behaviour corresponds to the enlargement of the active clamping zone as the crack extends. The steepness of the *R*-curve depends on the density of the clamping sites.

References

1. Das, S. & Curlee, T. R., The cost of silicon nitride powder and the economic viability of advanced ceramics. *Am. Ceram. Soc. Bull.*, **71**(7) (1992) 1103–11.
2. Ault, N. N. & Yeckley, R. L., Silicon nitride. *Am. Ceram. Soc. Bull.*, **71**(5) (1992) 816.
3. Wei, G. C. & Becher, P. F., Development of SiC-whisker-reinforced ceramics. *Am. Ceram. Soc. Bull.*, **64**(2) (1985) 298–304.
4. Shalek, P. D., Petrovic, J. J., Hurley, G. H. & Gac, F. D., Hot-pressed SiC whisker/Si_3N_4 matrix composites. *Am. Ceram. Soc. Bull.*, **65**(2) (1986) 351–6.
5. Champion, E., Goursat, P., Besson, J. L., Madigou, V., Monthioux, M. & Lespade, P., Microstructure, strength and toughness of Si_3N_4–SiC whisker composites. *Ceram. Eng. Sci. Proc.*, **13**(9–10) (1992) 732–9.
6. Li, C. & Yamanis, J., Super-tough silicon nitride with *R*-curve behavior. *Ceram. Eng. Sci. Proc.*, **10**(7–8) (1989) 632–45.
7. Salem, J. A., Choi, S. R. & Freedman, M. R., Mechanical behaviour and failure phenomenon of an in-situ toughened silicon nitride. *J. Mater. Sci.*, **27** (1992) 4421–8.
8. Choi, S. R., Salem, J. A. & Sanders, W. A., Estimation of crack closure stresses for in-situ toughened silicon nitride with 8 wt% scandia. *J. Am. Ceram. Soc.*, **75**(6) (1992) 1508–11.

9. Li, C., Lee, D. & Lui, S., *R*-Curve behavior for in-stiu reinforced silicon nitrides with different microstructures. *J. Am. Ceram. Soc.*, **75**(7) (1992) 1777–85.
10. Ekström, T. & Nygren, M., SiAlON ceramics. *J. Am. Ceram. Soc.*, **75**(2) (1992) 259–76.
11. Suttor, D. & Fischman, G. S., Densification kinetics in sintered silicon nitride. *J. Am. Ceram. Soc.*, **75**(5) (1992) 1063–7.
12. Ramachandran, N. & Shetty, D. K., Rising crack-growth-resistance (*R*-curve) behavior of toughened alumina and silicon nitride. *J. Am. Ceram. Soc.*, **74**(10) (1991) 2634–41.
13. Hwang, C. J., Yang, K., Beaman, D. & Klassen, H., Effect of silicon carbide addition on a self-reinforced silicon nitride. *Ceram. Eng. Sci. Proc.*, **13**(9–10) (1992) 1032–9.
14. Choi, S. R. & Salem, J. A., Strength, toughness and *R*-curve behavior of SiC whisker-reinforced composite Si_3N_4 with reference to monolithic Si_3N_4. *J. Mater. Sci.*, **27** (1992) 1491–8.
15. Debaig, C., Goursat, P. & Desmarres, J. M., European Patent Application Number 88400323.7, 1988.
16. Chatfield, C., Ekström, T. & Mikus, M., Microstructural investigation of alpha–beta yttrium sialon materials. *J. Mater. Sci.*, **21** (1986) 2297–307.
17. Lee, F. & Bowman, K. J., Texture and anisotropy in silicon nitride. *J. Am. Ceram. Soc.*, **75**(7) (1992) 1748–55.
18. Leterrier, Y., G'Sell, C. & Hiver, J. M., Analyse tridimentionnelle de l'orientation des fibres dans les composites à partir de micrographies électroniques à balayage. *Revue des Composites et des Matériaux Avancés*, **2**(2) (1992) 143–64.
19. Becher, P. F., Hsueh, C. H., Angelini, P. & Tiegs, T. N., Toughening behavior in whisker-reinforced ceramic matrix composites. *J. Am. Ceram. Soc.*, **71**(12) (1988) 1050–61.
20. Jain, L. K. & Wetherold, C., Effect of fiber orientation on the fracture toughness of brittle matrix composites, *Acta Metall. Mater.*, **40**(6) (1992) 1135–43.
21. Gazzara, C. P. & Messier, D. R., Determination of phase content of Si_3N_4 by X-ray diffraction analysis. *Am. Ceram. Bull.*, **56**(9) (1977) 777–80.
22. Zhang, S. C. & Cannon, W. R., Preparation of silicon nitride from silica. *J. Am. Ceram. Soc.*, **67**(10) (1984) 691–5.
23. Glandus, J. C. & Boch, P., Uncertainty on the mean strength and Weibull's modulus of an alumina batch as a function of the number of samples. *J. Mat. Sci. Lett.*, **3** (1984) 74–6.
24. Evans, A. G. & Charles, E. A., Fracture toughness determination by indentation. *J. Am. Ceram. Soc.*, **59**(7–8) (1976) 371–2.
25. Ponton, C. B. & Rawlings, R. D., Vickers indentation fracture toughness test—Part 1: review of literature and formulation of standardized indentation toughness equations. *Mat. Sci. Tech.*, **5** (1989) 865–72.
26. Proposal of '89 Fracture Toughness Testing, Japan Fine Ceramics Center, Atsuta-ku Nagoya, 456 Japan.
27. Srawley, J. E., Wide range stress intensity factor expressions for ASTM-E399 standard fracture toughness specimens. *Int. J. Fract. Mech.*, **12** (1976) 475–6.
28. Quinn, G. D., Salem, J., Bar-on, I., Cho, K., Foley, M. & Fang, H., Fracture toughness of advanced ceramics at room temperature. *J. Res. Natl. Stand. Technol.*, **97** (1992) 579–607.
29. Raj, R. & Bordia, R. K., Sintering behavior of bi-modal powder compacts. *Acta Metall.*, **32**(7) (1984) 1003–19.
30. Scherer, G. W., Sintering with rigid inclusions. *J. Am. Ceram. Soc.*, **70**(10) (1987) 719–25.
31. Wadsworth, I. & Stevens, R., The influence of whisker dimensions on the mechanical properties of cordierite/SiC whisker composites, *J. Eur. Ceram. Soc.*, **9**, (1992) 153–63.
32. Becher, P. F., Microstructural design of toughened ceramics. *J. Am. Ceram. Soc.*, **74**(2) (1991) 255–69.
33. Matsuhiro, K., & Takahashi, T., The effect of grain size on the toughness of sintered Si_3N_4. *Ceram. Eng. Sci. Proc.*, **10**(7–8) (1989) 807–16.
34. Nose, T. & Fujii, T., Evaluation of fracture toughness for ceramic materials by a single-edge-precracked-beam method. *J. Am. Ceram. Soc.*, **71**(5) (1988) 329–33.
35. Wieninger, H., Kromp, K. & Pabst, R. F., Crack resistance curve of alumina at high temperatures. *J. Mater. Sci.*, **22** (1987) 1352–8.
36. Braun, L. M., Bennison, S. J. & Lawn, B. R., Objective evaluation of short-crack toughness curves using indentation flaws: case study on alumina based ceramics. *J. Am. Ceram. Soc.* **75**(11) (1992) 3049–57.
37. Steinbrech, R., Growth of indentation cracks in Al_2O_3 under loading. Presented at the European Ceramic Society, Augsburg, FRG, 1991.